SIMULATIONS OF BEAM-WIRE EXPERIMENTS AT RHIC

Hyung Jin Kim*, Tanaji Sen†, FNAL, Batavia, IL 60563, USA

Abstract

A weak-strong beam simulation code (BBSIM) is used to study the compensation of long range beam-beam effects by current carrying wires at the Relativistic Heavy Ion Collider. Tune footprints and tune scans of diffusive aperture are presented for various wire separation distances. Beam life time is estimated using the dependence of the transverse diffusion coefficients on initial action. Comparison of the loss rate from tracking with that measured by BNL is presented.

INTRODUCTION

Long-range beam-beam interactions are known to cause beam loss in the Tevatron and they are expected to deteriorate beam quality in the LHC. Compensation of their effects has been proposed for the LHC. The test of this principle is now underway at RHIC [1]. Two current carrying wires, one for each beam, have been installed in the RHIC tunnel. First measurements of their impact on a beam are reported in reference [1]. In this report we discuss the results of numerical simulations of a wire acting on a beam with the parameters of RHIC. The aim is both to benchmark the simulations against the results reported so far and to predict the results of the compensation measurements to be done in the future.

MODEL

A beam-beam simulation code BBSIM has been developed at FNAL over the past few years. Results for wire experiments at the SPS and beam-beam experiments at RHIC were reported in references [2] and [3] respectively. The simulations reported here were also done with BBSIM which can track multi-particles and simulate nonlinear effects in a high energy circular accelerator. The following summarizes features of the package:

- 6D weak-strong model, includes synchrotron oscillations etc.
- Nonlinearities include chromaticity sextupoles, thin lens multipoles especially those in the IR quadrupoles at collision & current carrying wire.
- Head-on and Long-range interactions when present.
- Implementation by Fortran 90/95.
- Parallelization of I/O and computation.

* hjkim@fnal.gov
† tsen@fnal.gov

quantity	unit	value
gold energy	Gev/n	9.795
bunch intensity	10^9	0.7
emittance $\epsilon_{x,y}$(95%)	$mm\,mrad$	5.8
(β_x, β_y) at wire location	m	$(37, 124)$
(σ_x, σ_y) at wire location	mm	$(1.8, 3.4)$
tunes (ν_x, ν_y)		B $(28.230, 29.216)$
		Y $(28.220, 29.230)$
$(IL)_{max}$	Am	125
L_w	m	2.5
r_w	mm	3.5
wire separation	mm	12.8-24.8

Table 1: RHIC parameters at Au injection stage.

The effects of the strong beam on the *test* beam in a collider can be alleviated by using an appropriately placed current carrying wire with a well defined value of the current. In BBSIM, the integrated magnetic fields $B_{x,y}$ from the wire are found from [4]

$$\begin{pmatrix} B_x \\ B_y \end{pmatrix} = \frac{\mu_0 I_w}{4\pi} \frac{u - v}{x^2 + y^2} \begin{pmatrix} x \\ y \end{pmatrix}, \qquad (1)$$

where I_w is the current of wire compensator, u and v are $\sqrt{\left(\frac{3L_w}{2}\right)^2 + x^2 + y^2}$ and $\sqrt{\left(\frac{L_w}{2}\right)^2 + x^2 + y^2}$ respectively, and L_w the length of the wire. For cancelling the long-range beam-beam interactions with the wire, the integrated strength of the wire compensator should be commensurate with the integrated current of the beam bunch, i.e., $I_w L_w = ecN_b$, where N_b is the beam intensity. The parameters for RHIC long-range beam-beam compensators are listed in Table 1 [5].

SIMULATION RESULTS

As a first check of the simulations, we compare the zero amplitude tune shift from simulations with the analytical result. The transverse tune shifts at zero amplitude due to wire kicks [4] is given by

$$\Delta\nu_{x,y} = \pm \frac{\mu_0 I_w L_w}{8\pi^2 (B\rho)} \beta_{x,y} \frac{d_y^2 - d_x^2}{\left(d_y^2 + d_x^2\right)^2}, \qquad (2)$$

where $d_{x,y}$ denote the beam-wire distances normalized by RMS beam size at wire location in horizontal and vertical directions respectively, $I_w L_w$ the integrated strength of the wire, and $\beta_{x,y}$ the beta functions at wire location. The changes in the transverse tune as a function of the beam-wire separation distances is in good agreement with analytic relation, as shown in Fig. 1. The relative error of tune

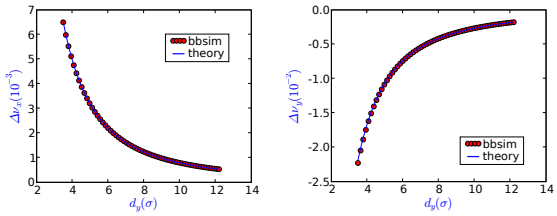

Figure 1: (Color) Tune shift dependence on the wire separation distance at zero amplitudes: (left) horizontal and (right) vertical tune shifts.

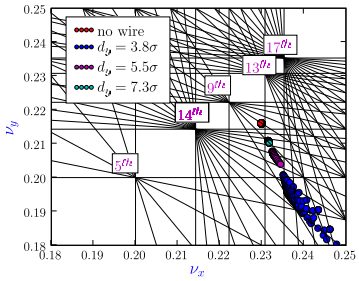

Figure 2: (Color) Tune footprints dependence on the wire separation distance for initial amplitudes up to 3σ.

shift between simulation and theory is less than 1%. The measured tune shifts in the recent experiments [1] are also in good agreement with analytical results.

Figure 2 presents tune footprints obtained by tracking single particles over 4096 turns and applying the FFT with a Hanning filter into the particle coordinates. The tune spreads are computed with start vertical and horizontal amplitudes up to 3σ and initial slopes set to zero. The red dots correspond to particles with no wire kicks so their tune is the beam base tune. The different colors correspond to different beam-wire distances. As the beam-wire separation decreases, the tune shifts get larger and the spreads get broader. For example at a separation of 3.8σ, the beam tune spread spans 5^{th}, 9^{th}, 13^{th}, and 14^{th} order resonances. At the larger separations shown here, the beam does not span the 5^{th} order resonances.

The results of dynamic aperture calculation are shown in Fig. 3. The particles are launched with equal vertical and horizontal emittances and with a distribution that neighboring particles differ in amplitude by half of RMS beam size.

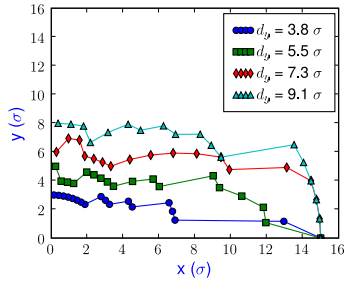

Figure 3: (Color) Dynamic aperture for $I_w = 50A$ and several different wire separations.

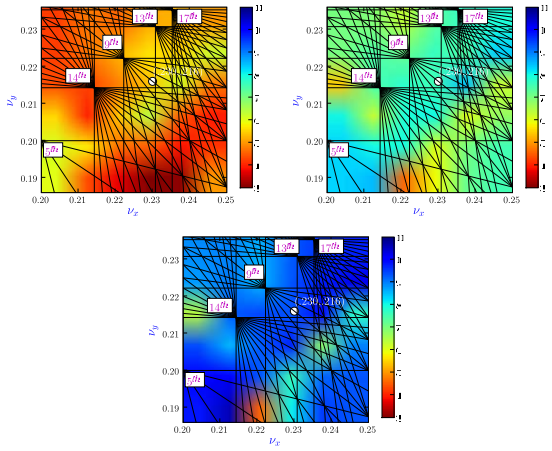

Figure 4: (Color) Tune scan for dynamic aperture for wire current $50A$: (top left) $d_y = 3.8\sigma$, (top right) $d_y = 5.5\sigma$, and (bottom) $d_y = 7.3\sigma$. Working point $(28.230, 29.216)$ is plotted as a white dot.

Net chromaticities in both planes are set to $\nu_x^{'} = -2$ and $\nu_y^{'} = -2$ using chromaticity sextupoles. The tunes are set to $Q_x = 28.230$ and $Q_y = 29.216$. Long-term tracking is carried out over 10^6 turns corresponding to 13 seconds storage time which is 20% of the RHIC injection period. The dynamic aperture of the machine is defined as the largest radial amplitude of particle that survives during the full 10^6 turns. In this simulation and in the experiments, the beam-wire separation is entirely in the vertical plane. From Fig. 3, the dynamic aperture is highly dependent on the angle of the wire position with the horizontal axis - particles launched with purely vertical amplitudes have smaller dynamic apertures than those launched along the horizontal. The dynamic aperture in the vertical plane is found to be linearly dependent upon the vertical separation d_y.

Figure 4 shows the contour plots of dynamic apertures over transverse tunes for three different wire separations. Red indicates low dynamic apertures around 3σ while blue indicates high dynamic apertures around 11σ. The tune scans are performed with increment $\Delta\nu = 0.01$ in transverse directions. It is found that at all wire separations, the largest dynamic apertures are distributed nearly along the diagonal, i.e., $\nu_x - \nu_y \simeq 0.02$. On the other hand, the zone along $\nu_x - \nu_y \simeq 0.03$ has the smallest dynamic apertures at all separations. This scan indicates that the nominal tune $(28.230, 29.216)$ is close to optimal. Furthermore, a sharper drop in dynamic aperture is observed near the 5^{th} resonance than at the other resonances as the separation drops from 7.3σ to 3.8σ.

The diffusion coefficients are calculated by loading 10^3 particles which have identical initial action in horizontal and vertical planes, and averaged over 10^3 consecutive turns to suppress action fluctuations. The diffusion coefficients can be calculated numerically from $D(J) = \frac{1}{M}\sum_{j=1}^{M} \lim_{N\to\infty} \left\langle (J(N) - J(0))^2 \right\rangle / N\big|_j$, where $J(0)$ is initial action, $J(N)$ action after N turns, and $\langle\rangle$ average over simulation particles. Figure 5 shows the simulated

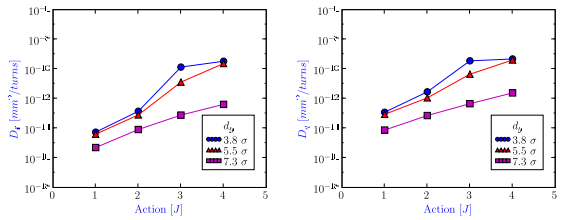

Figure 5: (Color) Diffusion coefficients as a function of initial action J for $I_w = 50A$: (left) horizontal and (right) vertical diffusion coefficients.

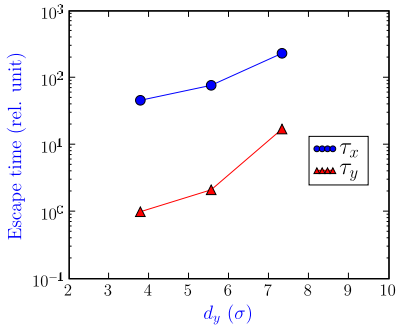

Figure 6: (Color) Lifetime normalized by τ_y at closest separation distance as a function of wire separations for $I_w = 50A$.

diffusion coefficients as a function of initial beam amplitudes and wire separations. The vertical axis is a logarithmic scale. It should be noted that dependence of diffusion coefficients upon initial action at a constant wire separation is clearly exponential even though there is small jump at $d_y = 3.8\sigma$. The jump may be caused by the direct interaction of the wire with particles which have commensurate amplitude with the separation distance. The diffusion decreases exponentially as the separation is increased at a constant initial action. Diffusion in the vertical direction is one-order higher than that in the horizontal due to the asymmetry of wire position. This is consistent with the significantly smaller dynamic aperture in the vertical plane shown above.

The characteristics of diffusion coefficients can be used in order to estimate the beam life time when the current carrying wire is present. From the diffusion equation, the escape time to an absorbing boundary at action J_A is given by

$$\tau_{\text{escape}} = \int_0^{J_A} J\, dJ/D\,(J)\ , \qquad (3)$$

where $D\,(J)$ is modeled by $D\,(J) = C\ \exp\,(-J/J_0)$ according to the result of Fig. 3. The escape time is interpreted as a measure of beam lifetime. In Fig. 6, the beam lifetimes in both vertical and horizontal directions are shown as a function of beam-wire separation. The lifetime is normalized by the vertical life time at smallest separation. The lifetime varies exponentially with the separation distance. A more exact estimate of the lifetime from the solution of the diffusion equation with the diffusion coefficients found above is in progress.

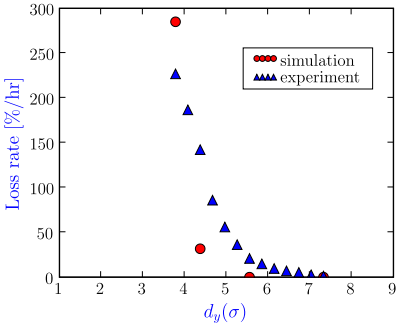

Figure 7: (Color) Comparison of the simulated beam loss rates with the measured [6] as a function of separations.

Figure 7 shows the result of long-term particle tracking, i.e., the beam loss rate calculation when wire compensator is present. The tracking is done with Gaussian beam distributions in transverse and longitudinal planes with 10^3 particles, and carried out over 10^7 turns for different wire separations with the wire current $I_w = 50A$. The loss rates are calculated by extrapolating the simulated loss rate from 10^7 turns to infinity. They are compared with the measured loss rates in Fig. 7. The loss rate at $d_y = 3.8\sigma$ is over-estimated compared with the measured one within few ten's percentage of error. On the other hand, the loss rate at $d_y = 5.5\sigma$ is under-estimated. Slight loss of particles is observed at $d_y = 7.3\sigma$ in the experiment, but not in the simulation. The simulation results need to be validated with larger number of particles to reduce the statistical error. There are also significant fluctuations in the measured loss rate at each separation but not shown here.

SUMMARY

A long-range beam-beam compensator at RHIC is studied at gold injection energy 9.795 Gev/n with a single wire in the blue ring. The results show that the dynamic aperture is highly dependent upon the angle between the wire and beam particles and mostly linearly dependent upon the separation. From the tune scan of dynamic aperture, the optimal working points are sought and verified. Dependence of beam lifetime on the separation is found to be exponential. Long-term tracking reveals that the simulated loss rate is reasonably consistent with the measured loss even with the small number of simulation particles.

REFERENCES

[1] W. Fischer, et al. this conference.

[2] F. Zimmermann, et al. PAC05 Proceedings, 686 (2004).

[3] W. Fischer, et al. EPAC06 Proceedings, 2158 (2006).

[4] B. Erdelyi and T. Sen, Fermilab-TM-2268-AD (2004).

[5] W. Fischer, et al. BNL C-A/AP/236 (2006).

[6] W. Fischer, et al. LARP Collaboration Meeting, Fermilab, April 18-20 (2007).